

Tăng cường khả năng ứng dụng chất nền carbon từ vỏ chuối kết hợp với g-C₃N₄ làm chất quang xúc tác xử lý môi trường

TÓM TẮT

Chất xúc tác quang carbon/g-C₃N₄ (BC/CN) được tổng hợp thành công bằng phương pháp nung đơn giản từ tiền chất carbon (tổng hợp từ vỏ chuối) và urea. Hoạt tính quang xúc tác và độ bền của vật liệu BC/CN được đánh giá qua sự phân hủy dung dịch RhB dưới vùng ánh sáng khả kiến. Ảnh hưởng của hàm lượng carbon trong composite trên hoạt tính xúc tác đã được khảo sát. Kết quả cho thấy hiệu suất quang xúc tác của composite BC/CN cao hơn g-C₃N₄ (CN) tinh khiết và so với các vật liệu composite ở các tỷ lệ khác. Điều này cho thấy vật liệu BC/CN-150 có độ bền quang xúc tác dưới vùng ánh sáng khả kiến. Kết quả này sẽ cung cấp cái nhìn mới về việc điều chế các chất xúc tác quang có hiệu quả cao trên nền g-C₃N₄.

Từ khóa: carbon, g-C₃N₄, chất xúc tác quang, rhodamine B, vỏ chuối.

Enhance the applicability of carbon substrates from banana peels combined with g-C₃N₄ as a photocatalyst for environmental treatment

ABSTRACT

Carbon/g-C₃N₄ photocatalyst (BC/CN) was successfully prepared by a simple calcination method from carbon precursor (synthesized from waste banana peels) and urea. The activity and stability of BC/CN were evaluated by rhodamine B (RhB) degradation under visible light. The influence of carbon content in the composite on catalytic activity was studied. The results show that the photocatalytic efficiency of the BC/CN composite is higher than that of the g-C₃N₄ (CN) pristine and the rate constant of the BC/CN-150 sample is higher than the other samples. This shows that BC/CN-150 material has photocatalytic stability under the visible light region. This process will provide new insight into preparing highly efficient g-C₃N₄-based photocatalysts.

Keywords: *carbon, g-C₃N₄, photocatalyst, rhodamine B, banana peels.*

1. INTRODUCTION

The rapid growth of the world's population, the constant progress of industrialization and the constant development of modern medicine have led to the release of large amounts of toxic and harmful substances into the environment. Finding green and sustainable technologies to solve these problems is urgent. Various methods are used to remove organic pollutants from water. However, the insufficient mineralization capacity of organic pollutants and the specific requirements for catalysts limit their practical application. Photocatalytic degradation of pollutants is commonly used due to its fast degradation rate and high mineralization¹. Therefore, developing efficient, abundant and sustainable photocatalysts is an important trend for heterogeneous media catalysis. As an important non-metallic material, graphite carbon nitride (g-C₃N₄) is characterized by many excellent features such as thermodynamic stability, suitable bandgap energy and high flexibility of polymers². However, the adjacent planes of g-C₃N₄ are initially stacked by Van der Waals force, which is not beneficial for charge carrier transfer and photocatalytic activity. The high photogenerated electron-hole recombination rate limits the photocatalytic process of the material³. Many methods have been proposed to adjust the morphological structure and surface chemical state of g-C₃N₄ to improve the photocatalytic efficiency of the material. One of the most used methods is to

combine with other materials to create composites such as MoS₂⁴, WO₃⁵, and SnS₂⁶.

Recently, it has been reported that carbon materials with sp² hybridized π bonds can suppress photogenerated electron-hole recombination and improve the utilization of visible light when combined with photoresists.⁷. The research group of Ong et al⁸ synthesized reduced graphene oxide (rGO)/g-C₃N₄ material through electrical interaction. With the excellent electrical conductivity and high electron storage capacity of graphene, photogenerated electrons transfer from g-C₃N₄ to rGO through an osmosis mechanism to improve the efficiency of CO₂ reduction into CH₄ by photocatalysis. The research group of Gu and his colleagues⁹ synthesized rGO/g-C₃N₄ material by microwave method from GO and melamine precursors. The results showed that the existence of rGO did not disrupt the structure of g-C₃N₄. The rate of decomposition of rhodamine B is 2.86 times that of g-C₃N₄ under visible light, this may be due to the more effective photogenerated electron-hole separation of the composite due to the synergistic effect of rGO and g-C₃N₄.

Besides, outstanding adsorption capacity is also very important in the photocatalytic degradation process in aqueous environment. Because nanostructured carbon materials have a great influence on the growth direction of the outer homogeneous phase, the microscopic morphology of the obtained C/g-C₃N₄ composites can also affect the ability to absorb

light, especially the absorbance of different wavelength ranges. Therefore, in this article, we study the effect of the ratio of synthesized carbon nanomaterials on the performance of photocatalytic degradation of RhB under visible light.

2. EXPERIMENTAL SECTION

2.1. Material synthesis

Chemicals: All chemicals for materials synthesis including banana peel, urea, KOH 20%, HCl 2M, C₂H₅OH, H₂O₂, and rhodamine B (China).

Materials synthesis:

Banana peels are washed with deionized water to remove dirt and cut into small pieces while still fresh. Then, it is dried in a vacuum environment for 24 hours at 110 °C. The dry shell is finely ground and calcined in an Argon gas at 800 °C for 5 hours, the heating rate is 5 °C/min. Then the obtained product is further treated with KOH 20% solution at 70 °C for 2 hours and HCl 2M solution at 60 °C for 15 hours. The obtained product is filtered, washed and dried in a vacuum environment at 110 °C for 12 hours. Next, the product is calcined in air at 300 °C for 3 hours. After calcination, the product is filtered, washed with HCl 2M solution and water, dried to obtain the product is activated carbon from banana peel, denoted BC.

The mixture of urea (20 g) with BC (0.1 g) was dispersed into 50 ml of water and alcohol solution and stirred continuously at a temperature of 60 °C until completely dry. Grind the solid amount finely and calcine in the Argon gas at 550 °C for 1 hour. The solid was filtered, washed and dried at 80 °C for 12 hours to obtain the C/g-C₃N₄ composite (symbolized as BC/CN). For comparison, the material g-C₃N₄ was also synthesized similarly to the above conditions but without the presence of activated carbon (symbolized as CN).

2.2. Material characterization

X-ray diffraction spectra of the samples were measured on a Bruker D2 Advance diffractometer with a Cu X-ray tube with wavelength λ (CuK α) = 1.5406 Å, power 40 kV, current 40 mA. Scanning angle from 10 to 80°. Infrared spectra were recorded on an IRAffinity-1S spectrometer (Shimadzu) with wavenumbers ranging from 400 to 4000 cm⁻¹. The composition of the element was determined by EDS spectroscopy. UV-Vis-DRS spectra of material samples were determined on a Jasco-V770

machine with wavelengths from 200 - 800 nm. TEM images were measured on a JEOL JEM-2100F.

2.3. Photocatalytic properties

The photocatalytic activity of the material was determined through the decomposition reaction of RhB in aqueous solution under visible light. Add 50 mg of catalyst into 100 mL of RhB solution with a concentration of 10 mg/L and stir in the dark for 1 hour to achieve adsorption-desorption equilibrium. Then, proceed with the photocatalytic process with a 30W LED lamp. Every 10 minutes, take 5 mL of the solution and centrifuge, removing the solid part. The concentration of RhB in the solution was determined on a UV-Vis meter (CE-2011) at a wavelength of 553 nm.

3. RESULTS AND DISCUSSION

3.1. Material characteristics

Characteristic results of the crystal structure of materials BC, CN and BC/CN-x (x=100, 150 and 200) were investigated by X-ray diffraction spectrum and the results are shown in Figure 1.

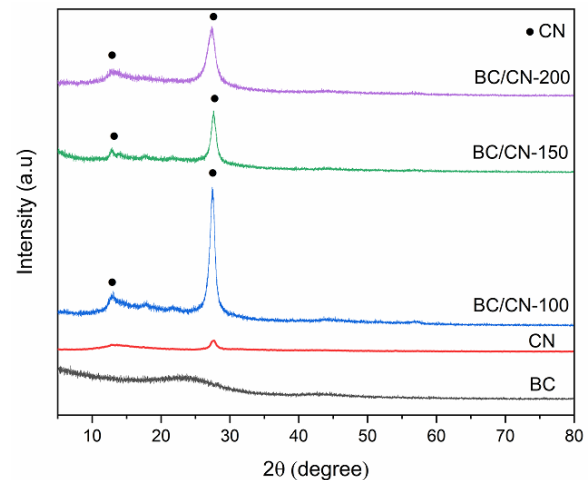


Figure 1. XRD patterns of BC, CN and BC/CN-x (x = 100; 150; 200)

The results in Figure 1 show that the BC sample has a raised area in the value range $2\theta = 20-30^\circ$, which is characteristic of the amorphous structure of activated carbon¹⁰. The CN sample has a diffraction peak at $2\theta = 13.2^\circ$ and 27.5° due to the layered structure of g-C₃N₄ with alternating stacking of conjugated aromatic units similar to the structure of graphite¹¹. In the BC/CN-x composite, all the peaks of g-C₃N₄ appeared but no peaks of the BC sample were seen. This may be due to the overlap of carbon layers between g-C₃N₄ crystals by composite formation.

The chemical bond characteristics of the samples were characterized by FT-IR spectroscopy, the results are shown in Figure 2.

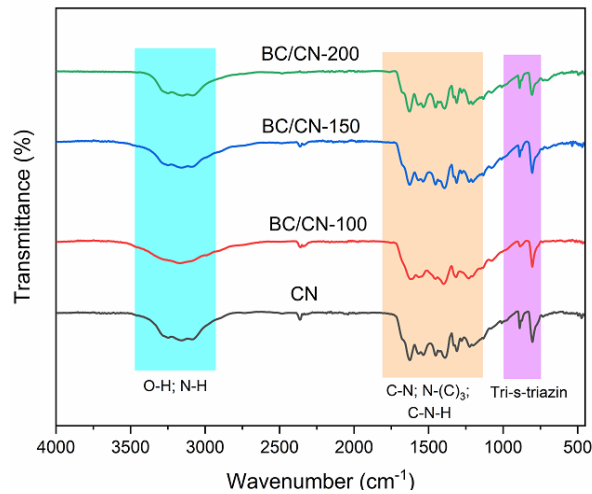


Figure 2. FT-IR spectra of CN and BC/CN-x ($x = 100, 150, 200$)

For the CN sample, the intensity band at 809.6 cm^{-1} shows the typical characteristic structure of tri-s-triazine¹². Bands at $1635.1, 1570.8$ and 1418.3 cm^{-1} are assigned to the aromatic C-N vibration. The bands at 1324.6 and 1254.9 cm^{-1} are assigned to the stretching vibrations of the bonded blocks of fully condensed N-(C)₃ and partially condensed C-N-H, respectively¹³. Absorbance in the range of $3200 - 3400\text{ cm}^{-1}$ is related to residual N-H groups and O-H bands¹⁴. Thereby, it is seen that there is no obvious change between the CN and the BC/CN-x, which shows that the presence of amorphous carbon does not change the structure of g-C₃N₄.

The structures of BC, CN and BC/CN composite are characterized by TEM images shown in Figure 3.

The TEM image of the BC sample (Figure 3a) shows a complex structure with defective graphene layers. The CN material (Figure 3b) has a morphology similar to a 2D nanosheet with a thin layer structure. However, compared to the 2D layered sheets of CN, the BC/CN (Figure 3c) shows stacked layers. This can be amorphous carbon materials grown on CN to form composites with surfaces in close contact with each other by heat treatment. The EDX spectrum of the composite shows the full elemental compositions of C and N (Figure 3d).

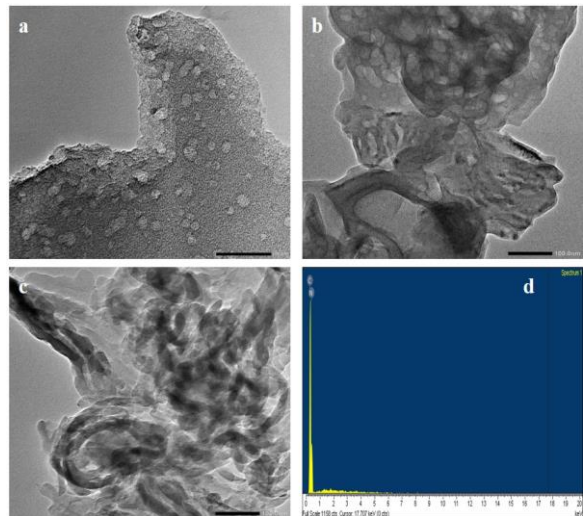


Figure 3. TEM image of BC (a); CN (b); BC/CN-150 (c) and EDX of BC/CN-150 (d)

To determine the photoelectric properties of CN and BC/CN-x composite, UV-Vis diffuse reflectance spectra were performed in Figure 4.

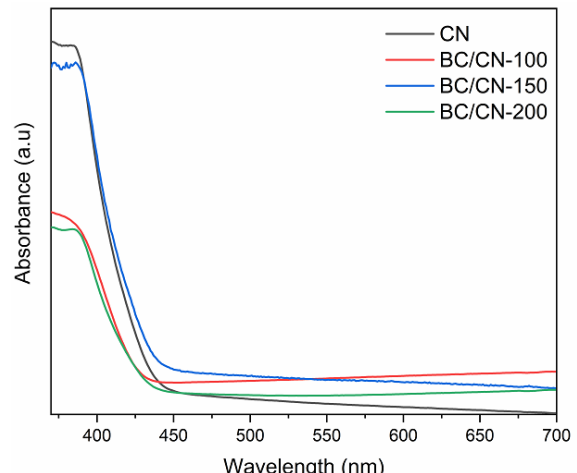


Figure 4. UV-vis diffuse reflectance spectra of CN; BC and BC/CN-x composite

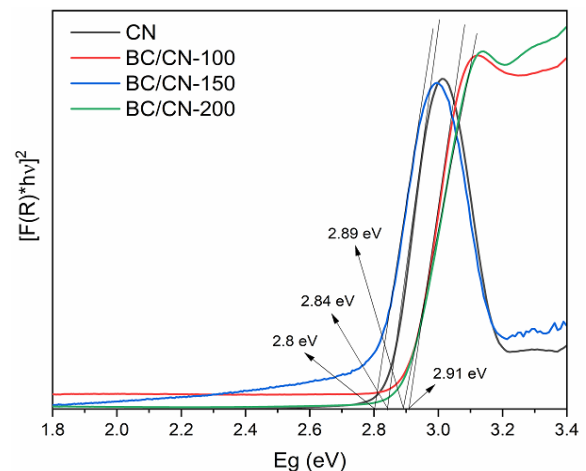


Figure 5. Band gap energy of CN and BC/CN-x composite

The results show that the composite after combining with amorphous carbon has a higher

absorption intensity over the wavelength range investigated. This is clearly shown in Figure 5 about the band gap of the material. In which the band gap of BC/CN-150 sample ($E_g=2.8$ eV) has a smaller value than the two other samples BC/CN-100 ($E_g=2.89$ eV); BC/CN-200 ($E_g=2.91$ eV) and CN pure ($E_g=2.84$ eV).

3.2. Photocatalytic properties of materials

BC; CN and BC/CN-x composites were investigated for their photocatalytic activity in decomposing RhB under visible light. The results are shown in figure 6. Before evaluating the photocatalytic efficiency, the samples were adsorbed in the dark for 60 minutes to reach the adsorption-desorption balance.

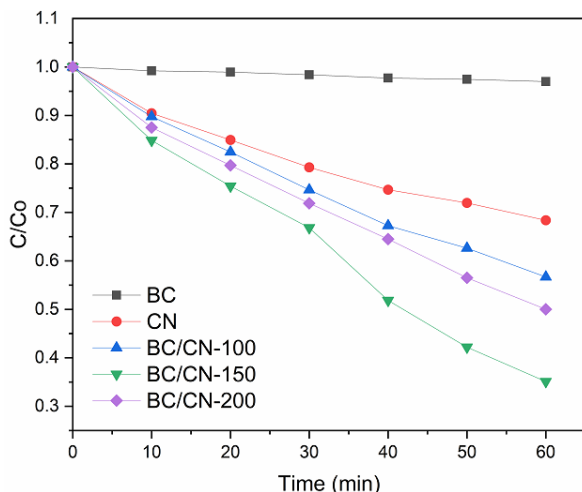


Figure 6. RhB decomposition under visible light of materials

Figure 6 shows CN; BC/CN-100; BC/CN-150 and BC/CN-200 have an efficiency of 32%; 43.3%; 65% and 50% respectively. This shows that composite have higher photocatalytic efficiency than simple materials. This may be because BC material acts as an agent that increases the electrical conductivity and photo-adsorption capacity in the visible light region of the composite, demonstrated through the UV-Vis DRS spectrum (Fig.4) and E_g value (Fig.5). The laws of photocatalytic kinetics of materials all comply with the Langmuir-Hinshelwood model (Figure 7).

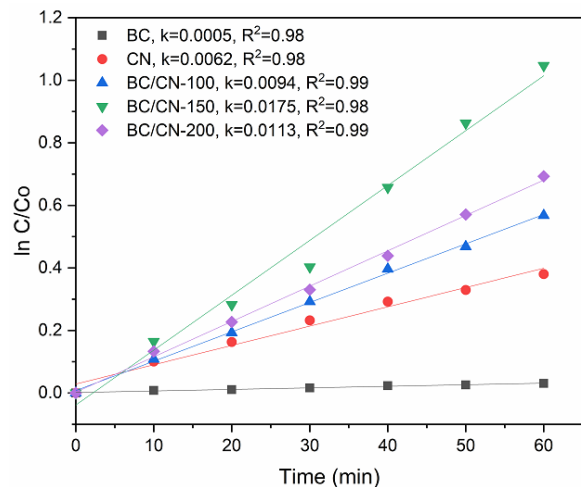


Figure 7. Kinetic fitting plot using the pseudo-first-order model of BC, CN and BC/CN-x composite

4. CONCLUSION

BC/CN-x composite with different ratios were successfully synthesized via a simple reduction heating method in an Argon atmosphere from urea and carbon precursors. In particular, carbon materials are synthesized from waste biomass raw materials of banana peels. The photocatalytic activity of the composite material BC/CN-150 ($H = 65\%$) is much higher than that of the $\text{g-C}_3\text{N}_4$ single ($H = 32\%$) for the decomposition of RhB after 60 minutes of reaction under the visible light region. Therefore, this shows that the presence of carbon significantly improves the photocatalytic efficiency of the materials. This is a promising new research direction in utilizing waste as materials for wastewater treatment and minimizing environmental pollution.

REFERENCES

1. Ruijie Yang, Y. Z., Yingying Fan, Renheng Wang, Rongshu Zhu, Yuxin Tang, Zongyou Yin, Zhiyuan Zeng, InVO₄-based photocatalysts for energy and environmental applications. *Chemical Engineering Journal* **2022**, 428, 131145.
2. Sakthivel Kumaravel, C. C., Govindasamy Palanisamy, Jintae Lee, Imran Hasan, Saranraj Kumaravel, Balakrishna Avula, Uma Devi Pongiya and Krishnakumar Balu, Highly Efficient Solar-Light-Active Ag-Decorated $\text{g-C}_3\text{N}_4$ Composite Photocatalysts for the Degradation of Methyl Orange Dye. *Micromachines* **2023**, 14, 1454.
3. Xinhe Wu, D. G., Ping Wang, Huogen Yu, Jiaguo Yu, NH₄Cl-induced low-temperature formation of nitrogen-rich $\text{g-C}_3\text{N}_4$ nanosheets with improved photocatalytic hydrogen evolution. *Carbon* **2019**, 153, 757-766.

4. Ha Tran Huu, M. D. N. T., Van Phuc Nguyen, Lan Nguyen Thi, Thi Thuy Trang Phan, Quoc Dat Hoang, Huy Hoang Luc, Sung Jin Kim & Vien Vo, One-pot synthesis of S-scheme $\text{MoS}_2/\text{g-C}_3\text{N}_4$ heterojunction as effective visible light photocatalyst. *Scientific Reports* **2021**, *11*, 14787.
5. Jie Meng, J. P., Zefang He, Shiyu Wu, Qingyun Lin, Xiao Wei, Jixue Lia and Ze Zhang, Facile synthesis of $\text{g-C}_3\text{N}_4$ nanosheets loaded with WO_3 nanoparticles with enhanced photocatalytic performance under visible light irradiation. *RSC Adv.* **2017**, *7*, 24097-24104.
6. Thanh Huong Nguyen Thi, H. T. H., Hung Nguyen Phi, Van Phuc Nguyen, Quoc Dat Le, Lan Nguyen Thi, Thi Thuy Trang Phan, Vien Vo, A facile synthesis of $\text{SnS}_2/\text{g-C}_3\text{N}_4$ S-scheme heterojunction photocatalyst with enhanced photocatalytic performance. *Journal of Science: Advanced Materials and Devices* **2022**, *7*, 100402.
7. Quanlong Xu, B. C., Jiagu Yu, Gang Liu, Making co-condensed amorphous carbon/ $\text{g-C}_3\text{N}_4$ composites with improved visible-light photocatalytic H_2 -production performance using Pt as cocatalyst. *Carbon* **2017**, *118*, 241-249.
8. Wee-Jun Ong, L.-L. T., Siang-Piao Chai, Siek-Ting Yong, Abdul Rahman Mohamed, Surface charge modification via protonation of graphitic carbon nitride ($\text{g-C}_3\text{N}_4$) for electrostatic self-assembly construction of 2D/2D reduced graphene oxide (rGO)/ $\text{g-C}_3\text{N}_4$ nanostructures toward enhanced photocatalytic reduction of carbon dioxide to methane. *Nano Energy* **2015**, *13*, 757-770.
9. Yongpan Gu, Y. Y., Jingye Zou, Tiantian Shen, Qinan Xu, Xiawei Yue, Jiang Meng, Jigang Wang, The ultra-rapid synthesis of rGO/ $\text{g-C}_3\text{N}_4$ composite via microwave heating with enhanced photocatalytic performance. *Materials Letters* **2018**, *232*, 107-109.
10. T. Van Thuan, B. T. P. Q., T.D. Nguyen, V.T.T. Ho, L.G. Bach, *Surf. Interfaces* **2017**, *6*, 209-217.
11. Md. R. Islam, A. K. C., M. A. Gafur, Md. A. Rahman, Md. H. Rahman, *Research on Chemical Intermediates* **2019**, *45*, 1753-1773.
12. J. Liu, T. Z., Z. Wang, G. Dawson, W. Chen, Simple pyrolysis of urea into graphitic carbon nitride with recyclable adsorption and photocatalytic activity. *J. Mater. Chem.* **2011**, *21*, 14398-14401.
13. X. Du, G. Z., Z. Wang, X. Wang, A scalable chemical route to soluble acidified graphitic carbon nitride: an ideal precursor for isolated ultrathin $\text{g-C}_3\text{N}_4$ nanosheets. *Nanoscale* **2015**, *7*, 8701-8706.
14. X. She, L. L., H. Ji, Z. Mo, Y. Li, L. Huang, et al., Template-free synthesis of 2D porous ultrathin nonmetal-doped $\text{g-C}_3\text{N}_4$ nanosheets with highly efficient photocatalytic H_2 evolution from water under visible light. *Appl. Catal. B: Environ.* **2016**, *187*.